

Optical biopsy of early gastroesophageal cancer by catheter-based reflectance-type laser-scanning confocal microscopy

Madoka Nakao, M.D.¹, Shigeto Yoshida, M.D.², Shinji Tanaka, M.D.²,
Yoshito Takemura, M.D.¹, Shiro Oka, M.D.², Masaharu Yoshihara, M.D.³,
Kazuaki Chayama, M.D.¹

¹Department of Medicine and Molecular Science, Division of Frontier Medical Science,
Programs for Biomedical Research, Graduate School of Biomedical Sciences,
Hiroshima University, Hiroshima, Japan

²Department of Endoscopy,
Hiroshima University Hospital, Hiroshima, Japan

³Department of Health Service Center,
Hiroshima University, Hiroshima, Japan

Address for correspondence:

Shigeto Yoshida, M.D., PhD

Department of Endoscopy,
Hiroshima University Hospital,

1-2-3 Kasumi, Minami-ku,

Hiroshima, 734-8551, Japan

Telephone: +81-82-257-5193

Facsimile: +81-82-257-5193

E-mail: yoshida7@hiroshima-u.ac.jp

Abstract

Magnified endoscopic observation of the gastrointestinal tract has become possible. However, such observation at the cellular level remains difficult. Laser-scanning confocal microscopy (LCM) is a novel, noninvasive optical imaging method that provides instant microscopic images of untreated tissue under endoscopy. We compared prototype catheter-based reflectance-type LCM images *in vivo* and histologic images of early gastroesophageal cancer to assess the usefulness of LCM in diagnosing such cancer. Twenty sites in the esophagus and 40 sites in the stomach were examined by LCM under endoscopy prior to endoscopic or surgical resection. A prototype catheter LCM system, equipped with a semiconductor laser that oscillates at 685 nm and analyzes reflected light (Mauna Kea Technologies, Paris, France; Fujinon, Saitama, Japan), was used *in vivo* without fluorescent agent. In all normal esophageal mucosa and esophageal cancers, the nuclei were visualized. In 9 of the 10 normal esophageal mucosa, cell membranes were visualized, and in 5 of the 10 esophageal cancers, cell membranes were visualized. In all normal gastric mucosa, nuclei and cell membranes were not visualized, but in 10 of the 20 gastric cancers, nuclei were visualized. This novel method will aid in immediate diagnosis under endoscopy without the need for biopsy.

Introduction

Detailed endoscopic observation of the esophagus, stomach, and colon has become possible due to advances in magnifying endoscopy and conventional endoscopy.^{1,2}

However, magnified observation at the cellular level remains difficult under endoscopic examination, thus often making histopathologic examination via biopsy a necessity.

Laser-scanning confocal microscopy (LCM) provides *in vivo* images that are close in quality to histopathologic images. This technology is currently being applied clinically in the field of gastroenterology. Most reports are of fluorescence-type LCM, which require a fluorescent agent.³⁻¹¹ Reflectance-type LCM, which does not need fluorescence, is in the investigational stage, and most reports are of *in vitro* studies.¹²

We compared *in vivo* LCM images and histologic images of early gastroesophageal cancer and normal mucosa to assess the usefulness of a newly developed prototype catheter-based reflectance-type LCM system (Mauna Kea Technologies, Paris, France; Fujinon, Saitama, Japan) for diagnosing gastroesophageal cancer.

Materials and Methods

Instrument specifications

We used a prototype LCM system equipped with a pulsed semiconductor laser centered at 685 nm. The combination of pulsed illumination (15 ns pulse width, 80 ns repetition

period) with a time-gated detection of the reflected light (15 ns detection window, 40 ns delay) permits to overcome the back-reflections onto the proximal optics by means of light travel-time differentiation.¹³ The flexible catheter probe was 2.6 mm in outer diameter and 3876 mm long (Fig. 1). The scanning field was 30,000 pixels-the number of fibers in the bundle and the frame rate was 12 images per second (Fig. 2). An objective with a numerical aperture of 1.2 was placed in contact with the tissue, with a focus of 30 μm from the objective lens, a lateral resolution of less than 1 μm , and an observation area 160 μm in diameter. The catheter probes were connected to the laser scanning unit and introduced under direct endoscopic visualization, LCM was performed after the flexible confocal catheter probe was introduced through the instrument channel of the endoscope (Fig. 3). All images of the LCM examinations were inspected, recorded, and stored digitally as real-time video sequences with the use of software on a PowerMac G5 Dual 1.8GHz personal computer (Apple Computer, Cupertino, CA, USA). In addition, still LCM images were saved for future review.

Patients and comparison of LCM images

Ten patients with esophageal cancer and 20 patients with gastric cancer underwent reflectance-type LCM examination after white-light endoscopic examination at Hiroshima University Hospital during the period April 2007 through July 2007. Clinical

characteristics of the lesions are presented in Table 1. The distal tip of the LCM catheter was placed gently against the mucosa, and an endoscopist captured LCM images of normal mucosa near the cancer and images of the cancer in the esophagus (normal mucosa, n = 10; cancer, n = 10) or stomach (normal mucosa, n = 20; cancer, n = 20). After endoscopic examination, a gastroenterologist (S.Y., who had analyzed LCM images previously) judged whether the cell nuclei and membranes were visible on the LCM images.¹² After these procedures, patients underwent endoscopic mucosal resection (EMR), endoscopic submucosal dissection (ESD), endoscopic aspiration mucosectomy (EAM), or surgery. The resected specimens were fixed in formalin, embedded in paraffin, sliced with a microtome, deparaffinized, and stained with hematoxylin-eosin for light microscopic examination. After these procedures, the histologic diagnosis was confirmed. The endoscopic system used in this study was a VP-4400 endoscope processor and an EG-590WR or EG-450D upper gastrointestinal endoscope (Fujinon). The study protocol conformed to the tenets of the Declaration of Helsinki and was approved by our institutional ethics committee.

Results

With the distal tip of the catheter placed gently against the mucosa and the cancer, real-time LCM images of the normal mucosa and of the cancer of the esophagus and

stomach were obtained safely and easily, and the influence of slight motion was ignore.

Even few water or blood was existed in the normal mucosa and cancer, the influence of water or blood was also ignore. The time required for scanning each normal and cancer site ranged between 16 and 390 seconds.

Normal esophageal mucosa

In LCM images of normal esophageal mucosa, high-reflectivity spots were observed near the center of honeycomb-like structures of high reflectivity. These high reflectivity spots and structures in the LCM images appeared to correspond to nuclei and cell membranes, respectively, in the histologic images of hematoxylin-eosin-stained sections (Fig. 4).

Esophageal cancer

In LCM images of esophageal cancer, high-reflectivity spots that were considered nuclei were observed. The nucleus-to-cytoplasm (N/C) ratio was much increased, and honeycomb-like structures of high reflectivity, considered cell membranes, were not observed (Fig. 5).

Normal gastric mucosa

In LCM images of normal gastric mucosa, cell membranes and nuclei were not visualized. However, the crypt cells were arranged like flower petals surrounding the

gastric pit (Fig. 6).

Gastric cancer

In LCM images of differentiated adenocarcinoma of the stomach, cell membranes were not visualized, and a disorganized configuration of glands with high-reflectivity spots that were considered nuclei was observed (Fig. 7). In LCM images of undifferentiated adenocarcinoma, no ductal structure was recognized; only an amorphous structure was seen. Cell membranes and nuclei were not visualized (Fig. 8).

Visualization of nuclei and cell membranes in LCM images in relation to histologic diagnoses is shown in Table 2. In all normal esophageal mucosa and esophageal cancers, the nuclei were visualized. In 9 of the 10 (90%) normal esophageal mucosa, cell membranes were visualized, and in 5 of the 10 (50%) esophageal cancers, cell membranes were visualized. In all normal gastric mucosa, nuclei and cell membranes were not visualized, but in 10 of the 20 (50%) gastric cancers, nuclei were visualized. The stroma was visualized as high reflectivity. In some cases, low-reflectivity spots were also observed in the LCM images which were considered mucin in goblet cells in the hematoxylin-eosin-stained specimen.

Discussion

Recent advances in endoscopic technology have afforded high-quality, detailed

diagnosis of gastrointestinal diseases. To confirm the presence of malignancy, however, snip biopsy is often performed under endoscopy when endoscopic examination reveals an abnormality. Thus, biopsy is performed for many lesions that are subsequently determined not be malignant. Histologic analysis of biopsy material remains the gold standard for the final diagnosis of a gastrointestinal lesion. Histologic diagnosis via biopsy involves the following process: formalin fixation of the specimen, cutting the specimen into small columns, paraffin embedding, ultra-thin slicing, deparaffinization, staining, glass slide, mounting, and finally light microscopic observation. Moreover, it takes several days to obtain a diagnosis. Also, snip biopsy is associated with bleeding, apparent endoscopic disappearance of cancer cells after biopsy, and artificial ulceration, which make endoscopic treatment, e.g. EMR, ESD, and EAM, difficult. In addition, because of the bleeding, biopsy cannot be easily performed in patients taking anticoagulants.

Being able to accurately image a lesion *in vivo* at the time of endoscopic examination without biopsy allows for prompt diagnosis and treatment. Fluorescence-type LCM is reported to be a promising tool for *in vivo* histopathologic examination during endoscopy and might overcome the disadvantages associated with conventional biopsy.³⁻¹¹ In recent years, there have been several reports describing the ability to

obtain an LCM image that corresponds precisely to the histopathologic tissue diagnosis in cases of gastrointestinal tract disease.³⁻¹² However, many of the reports were based on observations made on excised specimens or with fluorescence-type LCM. We too have previously used probe-based reflectance-type LCM to obtain images that are close to histopathologic specimens *in vitro*.¹² In the present study, however, we conducted examinations *in vivo* using catheter-based reflectance-type LCM, which enabled us to insert the microscope through the instrument channel of endoscope and to capture images at a single depth of 30 microns below the tissue surface. In our LCM observations of the esophagus, nuclei were detected at both sites of normal mucosa and cancer. In our LCM observations of the stomach, nuclei were not recognized in normal mucosa but were recognized in 50% of cancer sites. Because the slice of LCM was very thin, we assumed that the nuclei in the normal esophageal mucosa were easily visualized because the cells were composed of stratified squamous epithelial cells. Likewise, because the N/C ratio increased, we assumed that the nuclei of the esophageal cancer and gastric cancer were visualized, whereas the nuclei of the normal gastric mucosa were not visualized. Although further prospective and large number study, e.g., immediate diagnosis of neoplasia versus inflammation, is needed, we have shown that catheter-based reflectance-type LCM can provide images at the cellular level *in vivo*,

suggesting the possibility of immediate cancer diagnosis under endoscopic observation without the need for biopsy.

A fluorescence-type LCM system that uses a catheter was recently developed by Mauna Kea Technologies.³⁻⁸ This LCM system has the capability to provide dynamic (12 frames/second) ultrahigh resolution images at the cellular level on a field of view as wide as 260×260 μm with 1.5 lateral and 10-μm axial resolutions, at 60 μm working depth. To overcome the limits of the field of view, an image reconstruction algorithm that uses video mosaicing has been developed.³

One advantage of catheter-based LCM is that it allows the capture of an image during conventional endoscopic examination without changing to a specialized scope. The catheter-based reflectance-type LCM used in this study is of a size and flexibility to pass through the endoscopic instrument channel and to be placed accurately on the mucosa with guidance from the white-light endoscopic image. Furthermore, there is a report of *in vivo* acquisition of real-time and dynamic histologic images of the peritoneum, liver, and spleen during a novel, minimally invasive transgastric approach to surgery termed natural orifice transluminal endoscopic surgery (NOTES).⁴ Compared to reflectance-type LCM, fluorescence-type LCM can provide images with higher signal-to-noise ratios (although a fluorescence agent is needed). The fluorescence-type

LCM device used for diagnosing cancer,¹¹ visualizing lymphoepithelial lesions in gastric mucosa-associated lymphoid tissue-type lymphoma,⁵ detecting angiodysplasia,⁶ visualizing *Helicobacter pylori*,⁹ diagnosing lymphocytic colitis,⁷ diagnosing a dysplasia-associated lesional mass or adenoma-like mass in patients with ulcerative colitis,¹⁰ and for functional examinations that provide moving images with visualization of blood flow through microvessels.⁸ Unlike fluorescence-type LCM systems, reflectance-type LCM collects and counts the reflective laser beam and therefore requires no staining process. The fluorescence-type LCM requires some staining to obtain clear images, but the acquired image is of high quality, and signal-to-noise ratio is better than with the reflectance-type LCM. Further comparison of the two systems is needed but we believe that these two instruments complement each other.

In summary, this feasibility study showed that catheter-based reflectance-type LCM can be used in clinical practice to provide instant images that correspond well with hematoxylin-eosin-stained microscopic images. Therefore, we expect that this novel method will aid in immediate diagnosis under endoscopy without the need for biopsy.

Disclosure

System control software and prototype confocal catheter probes were provided on loan by Mauna Kea Technologies, Paris, France, and Fujinon, Saitama, Japan at no charge.

References

1. S. Nagata, S. Tanaka, K. Haruma, M. Yoshihara, K. Sumii, G. Kajiyama, and F. Shimamoto, "Pit pattern diagnosis of early colorectal carcinoma by magnifying colonoscopy: clinical and histological implications," *Int J Oncol.* 16(5), 927-934 (2000).
2. M. Hirata, S. Tanaka, S. Oka, I. Kaneko, S. Yoshida, M. Yoshihara, and K. Chayama, "Magnifying endoscopy with narrow band imaging for diagnosis of colorectal tumors," *Gastrointest Endosc.* 65(7), 988-995 (2007).
3. V. Becker, T. Vercauteren, C. H. von Weyhern, C. Prinz, R. M. Schmid, and A. Meining, "High-resolution miniprobe-based confocal microscopy in combination with video mosaicing (with video)," *Gastrointest Endosc.* 66(5), 1001-1007 (2007).
4. S. von Delius, H. Feussner, D. Wilhelm, A. Karagianni, J. Henke, R. M. Schmid, and A. Meining, "Transgastric in vivo histology in the peritoneal cavity using miniprobe-based confocal fluorescence microscopy in an acute porcine model," *Endoscopy.* 39(5), 407-411 (2007).

5. A. Morgner, M. Stolte, and S. Miehlke, "Visualization of lymphoepithelial lesions in gastric mucosa-associated lymphoid tissue-type lymphoma by miniprobe confocal laser microscopy," *Clin Gastroenterol Hepatol.* 5(9), e37 (2007).
6. A. Meining, M. Bajbouj, and R. M. Schmid, "Confocal fluorescence microscopy for detection of gastric angiodysplasia," *Endoscopy.* Epub ahead of print (2007).
7. A. Meining, S. Schwendy, V. Becker, R. M. Schmid, and C. Prinz, "In vivo histopathology of lymphocytic colitis," *Gastrointest Endosc.* 66(2), 398-399 (2007).
8. T. D. Wang, S. Friedland, P. Sahbaie, R. Soetikno, P. L. Hsiung, J. T. Liu, J. M. Crawford, and C. H. Contag, "Functional imaging of colonic mucosa with a fibered confocal microscope for real-time in vivo pathology," *Clin Gastroenterol Hepatol.* 5(11), 1300-1305 (2007).
9. R. Kiesslich, M. Goetz, J. Burg, M. Stolte, E. Siegel, M. J. Maeurer, S. Thomas, D. Strand, P. R. Galle, and M. F. Neurath, "Diagnosing *Helicobacter pylori* in vivo by confocal laser endoscopy," *Gastroenterology.* 128(7), 2119-2123 (2007).
10. D. P. Hurlstone, M. Thomson, S. Brown, N. Tiffin, S. S. Cross, and M. D. Hunter, "Confocal Endomicroscopy in Ulcerative Colitis: Differentiating

Dysplasia-Associated Lesional Mass and Adenoma-Like Mass,” *Clin Gastroenterol Hepatol.* 5(10), 1235-1241 (2007).

11. S. Kitabatake, Y. Niwa, R. Miyahara, A. Ohashi, T. Matsuura, Y. Iguchi, Y. Shimoyama, T. Nagasaka, O. Maeda, T. Ando, N. Ohmiya, A. Itoh, Y. Hirooka, and H. Goto, “Confocal endomicroscopy for the diagnosis of gastric cancer in vivo,” *Endoscopy.* 38(11), 1110-1114 (2006).

12. S. Yoshida, S. Tanaka, M. Hirata, R. Mouri, I. Kaneko, S. Oka, M. Yoshihara, and K. Chayama, “Optical biopsy of GI lesions by reflectance-type laser-scanning confocal microscopy,” *Gastrointest Endosc.* 66(1), 144-149 (2007).

13. A. Osdoit, M. Genet M, A. Perchant, S. Loiseau, B. Abrat, and F. Lacombe, “In vivo fibered confocal reflectance imaging: totally non-invasive morphological cellular imaging brought to the endoscopist (Proceedings Paper),” *Endoscopic Microscopy (Proceedings Volume).* 6082, 29-38 (2006).

Figure legends

Fig. 1. Catheter-based reflectance-type laser-scanning confocal microscope (Mauna Kea Technologies, Paris, France; Fujinon, Saitama, Japan).

Fig. 2. Schema of the catheter-based reflectance-type laser-scanning confocal microscopy.

Fig. 3. LCM examination for early gastric cancer under endoscopy.

Fig.4. Images of normal esophageal mucosal. a, Laser-scanning confocal microscopy image. b, Hematoxylin-eosin-stained tissue from the same specimen.

Fig. 5. Images of esophageal cancer. a, Laser-scanning confocal microscopy image. b, Hematoxylin-eosin-stained tissue from the same specimen.

Fig. 6. Images of normal gastric mucosa. a, Laser-scanning confocal microscopy image. b, Hematoxylin-eosin-stained tissue from the same specimen.

Fig. 7. Images of differentiated adenocarcinoma of the stomach. a, Laser-scanning confocal microscopy image. b, Hematoxylin-eosin-stained tissue from the same specimen.

Fig. 8. Images of undifferentiated adenocarcinoma of the stomach. a, Laser-scanning confocal microscopy image. b, Hematoxylin-eosin-stained tissue from the same specimen.

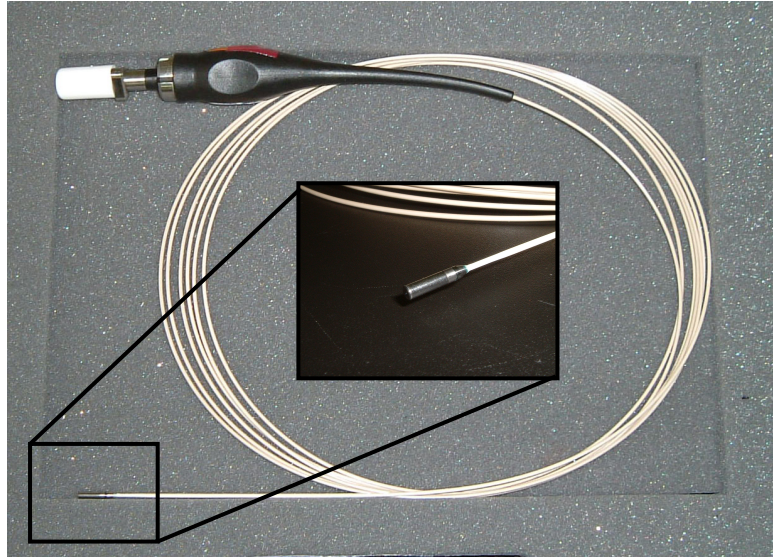


Fig. 1

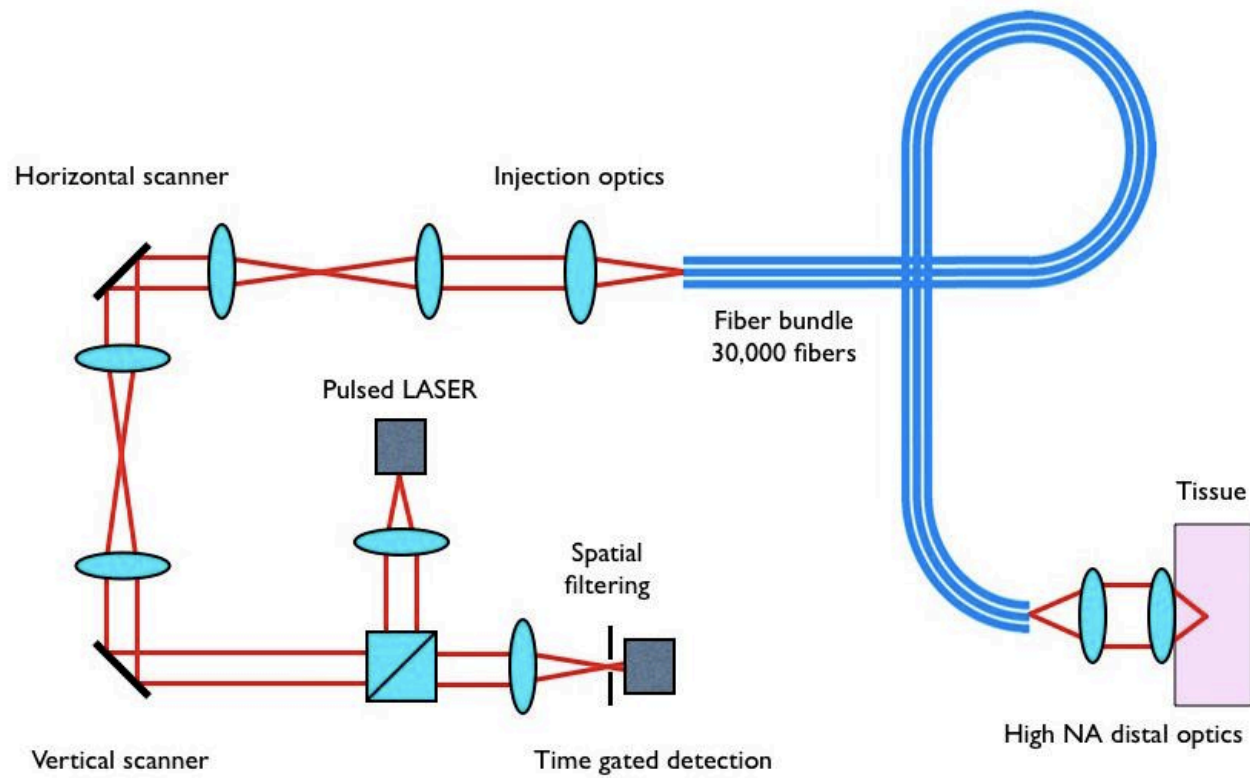


Fig. 2

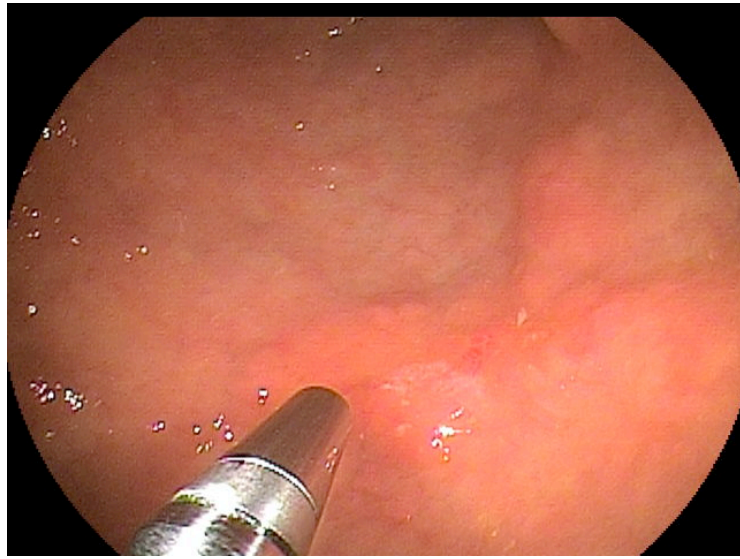


Fig. 3

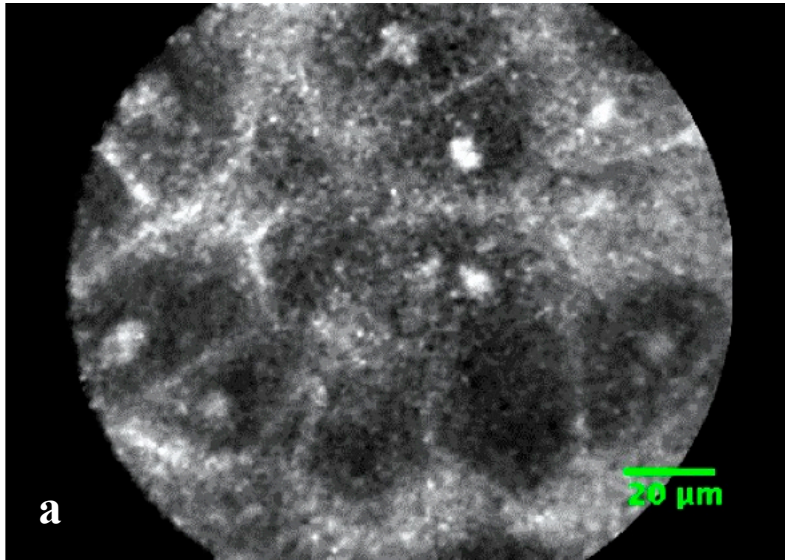


Fig. 4a

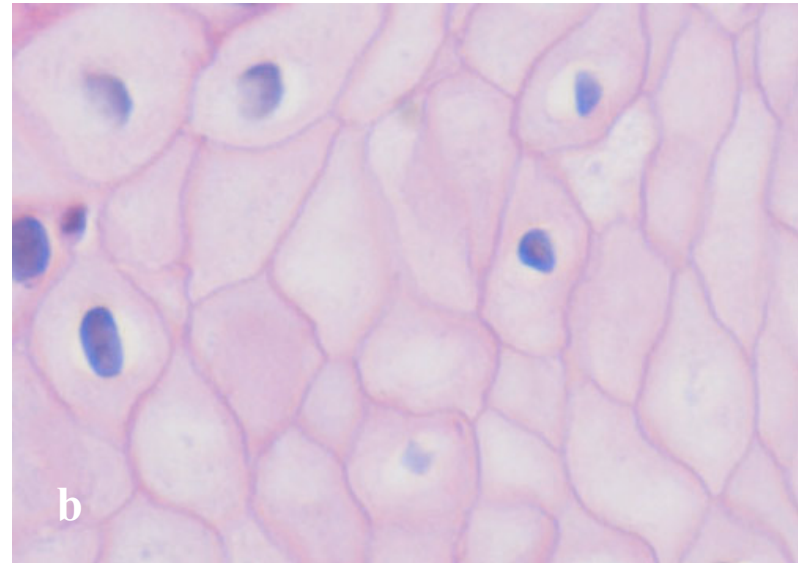


Fig. 4b

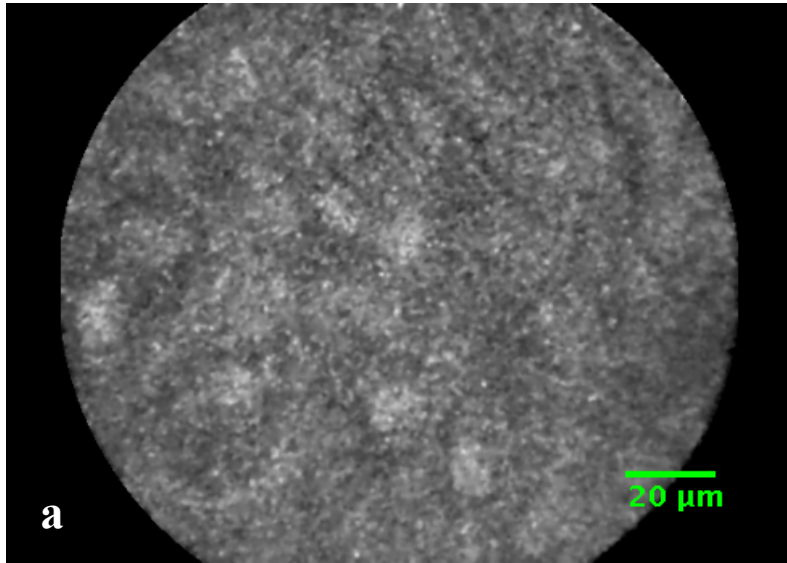


Fig. 5a

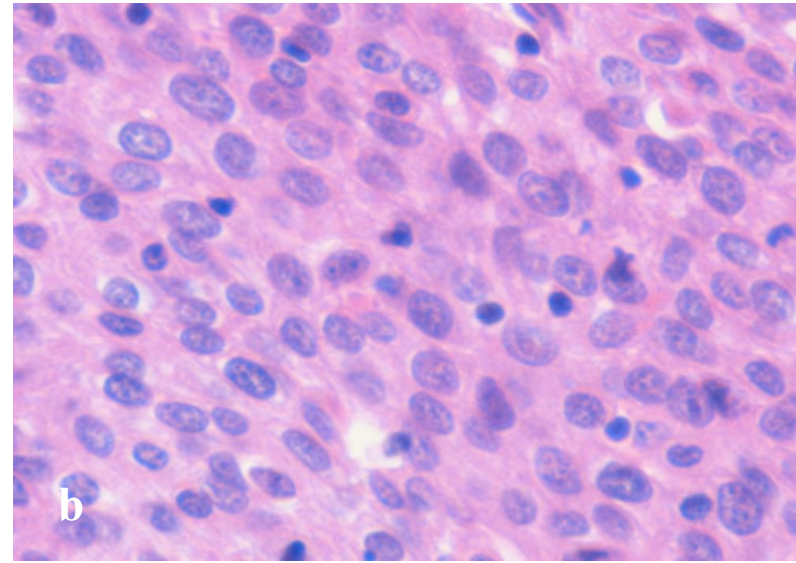


Fig. 5b

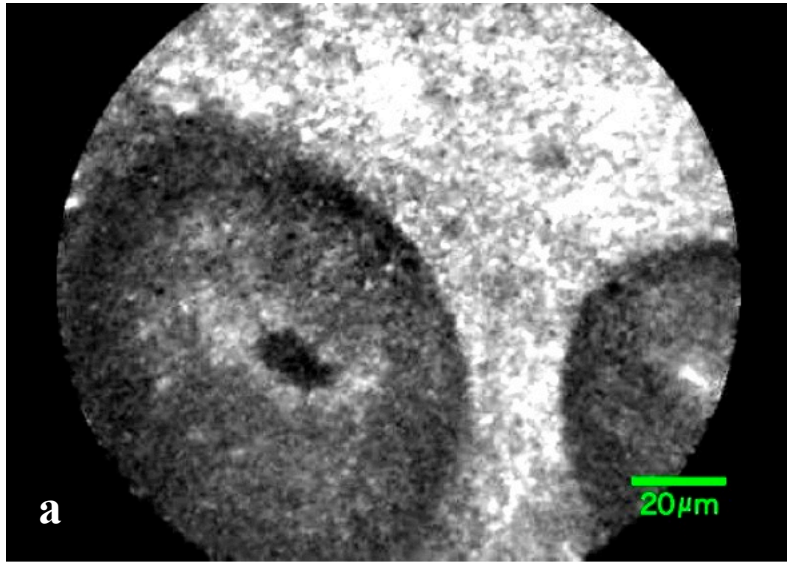


Fig. 6a

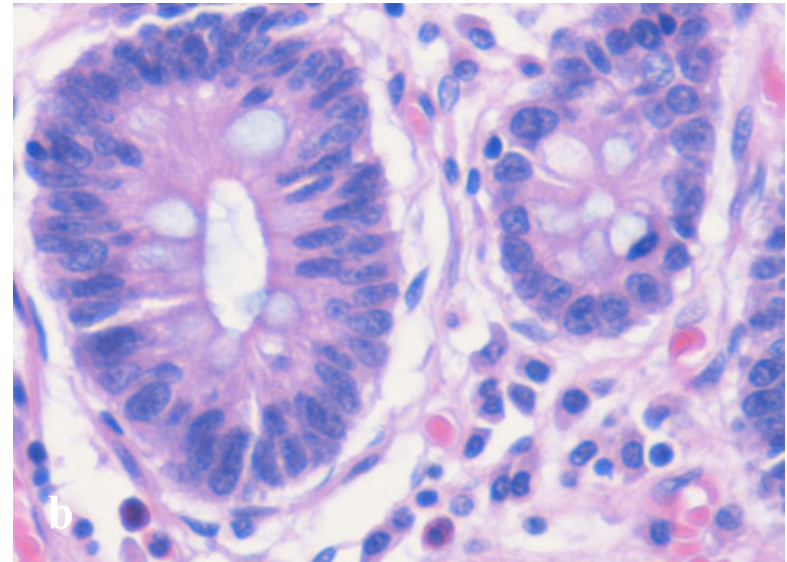


Fig. 6b

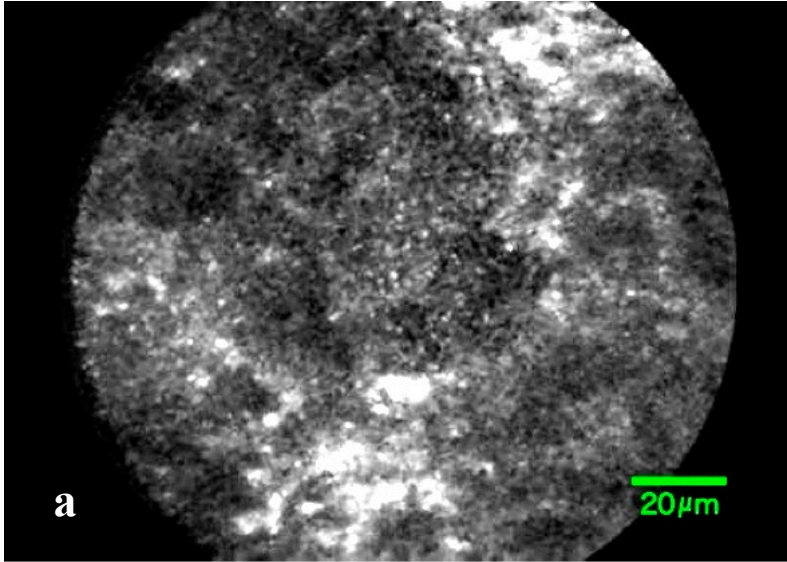


Fig. 7a

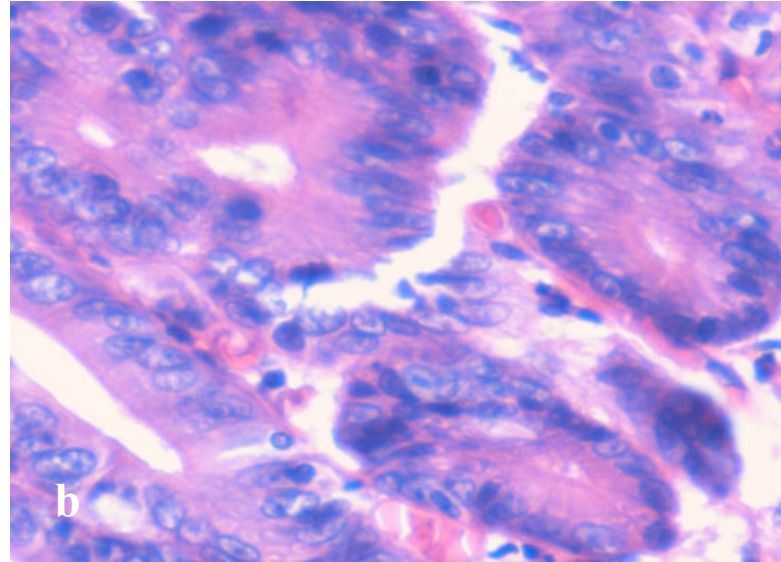


Fig. 7b

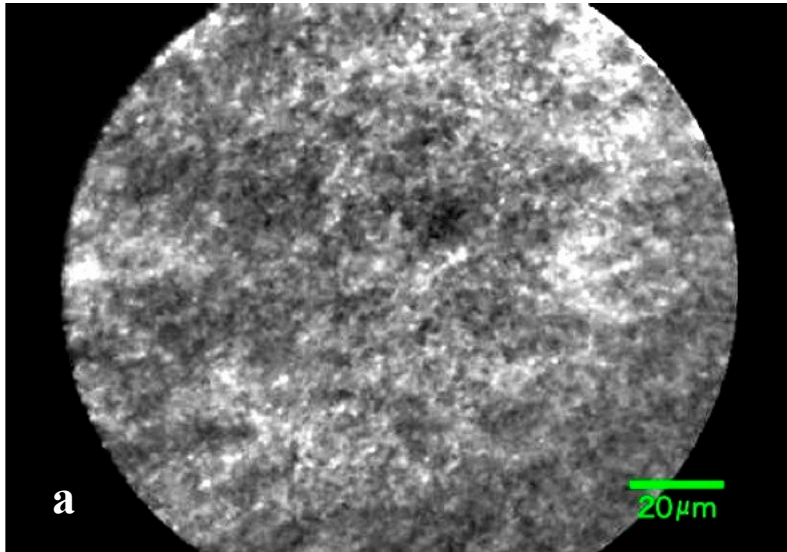


Fig. 8a

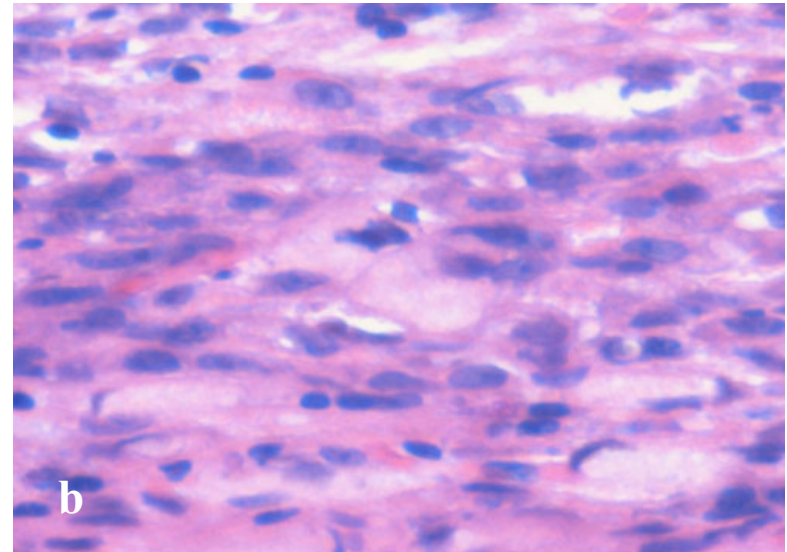


Fig. 8b

Table 1. Clinical Characteristics of the lesions

Esophagus		Stomach	
Tumor size (mm)		Tumor size (mm)	
Mean	22.8±7.5	Mean	16.3±10.5
Range	8-35	Range	10-35
Localization of tumor		Localization of tumor	
Esophagus	10	Antrum	6
		Angle	0
		Corpus	12
		Cardia	2
Depth of invasion		Depth of invasion	
Mucosa	10	Mucosa	13
Submucosa	0	Submucosa	7
Histologic type		Histologic type	
Squamous cell carcinoma	10	Well	10
		Moderately	6
		Papillary	1
		Poorly	1
		Signet ring cell	2

Table 2. Visualization of nuclei and cell membrane in LCM images in relation to histologic diagnoses

Histologic diagnosis	Nucleus	Cell membrane
Normal esophageal mucosa (n=10)	10 (100)	9 (90)
Esophageal cancer (n=10)	10 (100)	5 (50)
Normal gastric mucosa (n=20)	0 (0)	0 (0)
Gastric cancer: well (n=10)	6 (60)	0 (0)
moderately (n=6)	4 (66.7)	0 (0)
papillary (n=1)	0 (0)	0 (0)
poorly (n=1)	0 (0)	0 (0)
signet ring cell (n=2)	0 (0)	0 (0)

Number (and percentage) of samples are shown